Quadrupolar Hyperfine Anisotropy in $Fe(NH_4SO_4)_2 \cdot 6H_2O$ and Its Comparison with the Magnetic Susceptibility*

R. INGALLS
Department of Physics, University of Washington, Seattle, Washington
AND
K. ÔNO† AND LOUIS CHANDLER‡
Department of Physics, University of Illinois, Urbana, Illinois
(Received 11 January 1968)

An experiment to measure the quadrupolar hyperfine anisotropy, that is, the intensity ratio of the members of the quadrupole doublet in the Fe^{57} Mössbauer spectrum for ferrous ammonium sulfate, is reported. Measurements were carried out at 300 and 4.2°K with thin slabs of single crystals. Analysis of the data yields results in accord with a positive value of the principal electric-field-gradient (EFG) tensor component q, and values of the asymmetry parameter η of 0.7 at 300°K and 0.3 at 4.2°K. The orientation of the EFG axes of the two Fe^{2+} sites is also determined and related to the crystal axes. The quadrupolar data are also explained reasonably well in terms of a rhombic crystal field for the Fe^{2+} ion. The results are then used to explain in some detail the observed principal susceptibility data. It is explained why a tetragonal model works well in describing the magnetic susceptibility at temperatures above 20°K, even though it does not for the quadrupolar data. Finally, it is found that the local EFG and susceptibility axes do not coincide, presumably because the crystal-field symmetry is lower than rhombic, as a result of the dipole moments on the neighboring water molecules.

I. INTRODUCTION

IN this work we report on Mössbauer experiments aimed at examining in some detail the nature of the symmetry and orientation of the $3d$ electron distribution on the Fe^{2+} ion in monoclinic ferrous ammonium sulfate (FAS). The present work may be regarded as the sequel to earlier work on the specific heat,[1] susceptibility,[2–4] and quadrupole splitting[5] in the same compound. The specific-heat study by Hill and Smith[1] clearly exhibited an anomaly of the Shottky type, indicating a crystal-field splitting between the ground and first excited states of approximately 6.5 cm^{-1}. The susceptibility studies by Jackson[2] and later by Ohtsuka *et al.*[3] at lower temperatures showed that the spin $S=2$ was essentially free at room temperatures but approached the quenched state at temperatures below 10°K. The latter behavior required a singlet ground state and a crystal field at the ferrous ion which was of rhombic symmetry or lower. Ohtsuka[3] and also Bose *et al.*[4] have shown that a Hamiltonian with tetragonal symmetry works above 20°K, but the latter showed that the resulting crystal-field splitting parameter must have an extreme temperature dependence if it is to give the correct susceptibility between 20 and 300°K. In addition, the Mössbauer results[5] on the divalent iron-57 quadrupole splitting in powdered FAS have been shown to require rhombic, or lower, crystal-field symmetry as well. All these previous studies have neglected consideration of the orientation of the crystal-field axes in relation to the crystal axes, although Krishnan *et al.*[6] have given the orientation of the principal susceptibility axes.

The present work reports the quadrupolar hyperfine anisotropy, that is, the relative intensities of the members of the quadrupole doublet of the Mössbauer absorption spectrum, for many different angles in single crystals of FAS. This study, the preliminary results of which have been given earlier,[7] is quite similar to previous studies on monoclinic $FeCl_2 \cdot 4H_2O$.[8,9] We also consider the orientation and symmetry of the crystal field, within certain limits, by deducing the orientation of the electric-field-gradient (EFG) and susceptibility axes. We do this within the framework of a rhombic model, although from its shortcomings it is clear that a more complex model of lower symmetry is required to adequately account for the experimental results.

II. EXPERIMENT

Single crystals of FAS were grown at room temperature from a saturated solution. Slabs of the crystal were cut to include the a-c plane as well as the b axis at angle spacings of 20°. This was accomplished with a copper disk and carborundum suspended in cutting oil. The slabs were hand polished to a thickness of 0.18 mm.

Conventional Mössbauer equipment with a multichannel analyzer in the time mode was used. Data were taken at room temperature and at 4.2°K. The

* Supported in part by the U. S. Office of Naval Research and the National Aeronautics and Space Administration.
† Present address: Institute for Solid State Physics, University of Tokyo, Tokyo, Japan.
‡ Present address: Radiation Science Center, Rutgers University, New Brunswick, N. J.
[1] R. W. Hill and P. L. Smith, Proc. Phys. Soc. (London) **A66**, 228 (1953).
[2] L. C. Jackson, Phil. Trans. Roy. Soc. London **A224**, 1 (1924).
[3] T. Ohtsuka, H. Abe, and E. Kanda, Sci. Rept. Tohoku Univ. **9A**, 476 (1957).
[4] A. Bose, A. S. Chakravarty, and R. Chatterjee, Proc. Roy. Soc. (London) **A261**, 207 (1961).
[5] R. Ingalls, Phys. Rev. **133**, A787 (1964).
[6] K. S. Krishnan, N. C. Chakravarty, and S. Banerjee, Phil. Trans. Roy. Soc. London **A232**, 99 (1933).
[7] R. Ingalls, K. Ôno, and L. Chandler, Bull. Am. Phys. Soc. **12**, 901 (1967).
[8] P. Zory, Phys. Rev. **140**, A1401 (1965).
[9] K. Ôno (to be published).

TABLE I. Experimental results for the quadrupolar hyperfine anisotropy R, the intensity ratio of the members of the Fe^{57} quadrupolar doublet: $R=a_h/a_l$. The orientation angles (deg) are defined in Fig. 1. The angles Φ are measured with respect to the c axis. The data are accurate to about $\pm 5\%$.

Θ	Φ		R(300°K)	R(4.2°K)
0	0	(b axis)	1.15	1.10
90	−77	(a-c plane)	1.00	0.96
90	−57		1.56	1.50
90	−36		1.90	1.88
90	−17		1.73	1.62
90	9		0.99	1.06
90	23		0.68	0.82
90	43		0.46	0.55
90	63		0.46	0.53
90	83		0.61	0.67

cryostat was first cooled to nitrogen temperature slowly, before transferring the liquid helium, so that the sudden temperature change would not crack the sample. The geometry was aligned with an optical method after cooling down to the liquid-helium temperature.

A Mössbauer spectrum exhibiting an anisotropic quadrupole doublet was obtained for each orientation angle and temperature. The data were reduced by a least-squares analysis to yield the quadrupolar hyperfine anisotropy R, namely, the ratio of the area of the higher-energy member to that of the lower: $R=a_h/a_l$. The data are given in Table I, and the various orientation angles are defined in Fig. 1.

III. ANALYSIS

For an absorber in which all iron-57 nuclei are in identical sites, Zory[8] has shown the ratio of absorption cross sections to be

$$R(\Theta,\Phi)=\sigma_h(\Theta,\Phi)/\sigma_l(\Theta,\Phi)=[4\pm\Delta(\Theta,\Phi)]/[4\mp\Delta(\Theta,\Phi)], \quad (1)$$

where

$$\Delta(\Theta,\Phi)=(1+\tfrac{1}{3}\eta^2)^{-1/2}(3\cos^2\Theta-1+\eta\sin^2\Theta\cos2\Phi)=4(R-1)/(R+1). \quad (2)$$

In the latter expression, η is the asymmetry parameter of the EFG tensor, and the $\pm$ sign in the former expression corresponds to the sign of the principal value of the EFG tensor q. The angles Θ and Φ are measured with respect to the EFG axes x_q, y_q, and z_q. Thus, in the limit of a thin absorber, the absorption areas $a(\Theta,\Phi)$ are proportional to the cross sections, so that

$$R(\Theta,\Phi)\cong a_h(\Theta,\Phi)/a_l(\Theta,\Phi). \quad (3)$$

Thus, in this simple case, $\Delta(\Theta,\Phi)$, and hence η, may in principle be obtained through Eq. (2).

In FAS the iron ions are situated at two inequivalent sites related by reflection in the a-c plane[10] (Fig. 1). As shown in the Appendix, Eq. (1) is still valid for this case except that the expression for $\Delta(\Theta,\Phi)$ is more complicated, namely,

$$\Delta(\Theta,\Phi)=(1+\tfrac{1}{3}\eta^2)^{-1/2}[A(3\cos^2\Theta-1)+B\sin^2\Theta\cos2\Phi], \quad (4)$$

where

$$A=1-\tfrac{1}{2}\cos^2\alpha(3+\eta\cos2\beta) \quad (5)$$

and

$$B=[\eta\cos2\beta-\tfrac{1}{2}\cos^2\alpha(3+\eta\cos2\beta)]\cos2\gamma_q-\eta\sin\alpha\sin2\beta\sin2\gamma_q, \quad (6)$$

and α, β, and γ_q are the orientations of the local-field-gradient axes with respect to a set of principal axes in the crystal. The symmetry of the problem requires that the Z axis lie along the crystalline b axis and that the X, Y axes which lie in the a-c plane are so defined that $\Delta(\Theta,\Phi)$ takes the simple form in Eq. (4), i.e.,

$$\tan2\gamma_q\equiv\frac{-\eta\sin\alpha\sin2\beta}{\eta\cos2\beta-\tfrac{1}{2}\cos^2\alpha(3+\eta\cos2\beta)} \quad (7)$$

(see Appendix). Thus, in the limit of a thin absorber, Eqs. (1), (3), and (4) yield[11]

$$(1+\tfrac{1}{3}\eta^2)^{-1/2}A=\tfrac{1}{2}\Delta(0,0)=2(R-1)/(R+1)\,|_{b\text{ axis}} \quad (8)$$

and

$$(1+\tfrac{1}{3}\eta^2)^{-1/2}(-A+B\cos2\Phi)=\Delta(\tfrac{1}{2}\pi,\Phi)=4(R-1)/(R+1)\,|_{a\text{-}c\text{ plane}}. \quad (9)$$

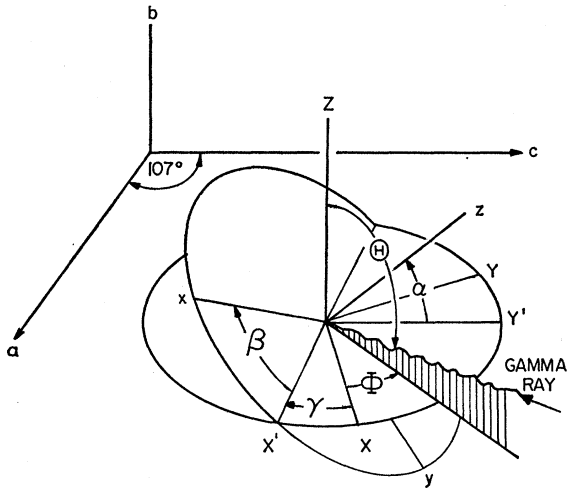

FIG. 1. Axes and angles used in this paper. The Mössbauer γ ray was incident along the $b(Z)$ axis, $\Theta=0$, as well as at many angles Φ in the a-$c(XY)$ plane, $\Theta=\frac{1}{2}\pi$. The set of local axes (x, y, z) is attached to one of the two Fe^{2+} sites, while (X, Y, Z) are principal axes determined by experiment. In the text, axes with the subscript q refer to the quadrupolar axes, while those labeled s refer to the susceptibility. (Second site not shown.)

[10] H. Montogomery, R. V. Chastain, J. J. Natt, A. M. Witkowska, and E. C. Lingafelter, Acta Cryst. **22**, 775 (1967).

[11] P. Zory (Ref. 8) has shown that for the directions of special symmetry, $\parallel$ or $\perp$ to the b axis, the recoilless fraction, which may be anisotropic, cancels in the area ratio, Eq. (3). Elementary considerations based on Ref. 8 also show that an approximate finite thickness correction may be accomplished by dividing the right-hand side of Eqs. (8) and (9) by the factor $1-x/8$, where x is the effective absorber thickness. We estimate this factor to be approximately unity at 300°K and 0.95 at 4.2°K because of the increased recoilless fraction.

In Fig. 2, we graph the experimental values of $4(R-1)/(R+1)$ for absorption in the a-c plane (i.e., perpendicular to slabs containing the b axis) and compare it with a curve determined by a least-squares fit. The agreement is quite reasonable, and gives the following results:

$$(1+\tfrac{1}{3}\eta^2)^{-1/2}A = 0.05\pm0.06, \quad T=4.2°\text{K}$$
$$= 0.15\pm0.06, \quad T=300°\text{K}$$
$$(1+\tfrac{1}{3}\eta^2)^{-1/2}B = 1.25\pm0.10, \quad T=4.2°\text{K}$$
$$= 1.40\pm0.10, \quad T=300°\text{K}.$$

We also find that the principal X axis of the quadrupolar hyperfine anisotropy lies at approximately $-32°$ and $-36°$ with respect to the c axis at 4.2 and 300°K, respectively.

The problem of determining the parameters α, β, γ_q, and η solely from the above results is in general very difficult, as is apparent from Eqs. (5) and (6). To attempt a solution we may start by assuming that α and β are unchanged with temperature. We also are guided by approximate values of η from other works,[12,13] namely, $\eta\cong0.7$ at $T=300°$K and $\eta\cong0$ at $T=4.2°$K. The parameter q has been found to be positive. Fortunately, we are able to get consistent results with the following parameters:

$$\alpha\cong32°, \quad \beta\cong100°, \quad \gamma_q\cong87°;$$
$$\eta\cong0.7 \text{ at } 300°\text{K} \text{ and } \eta\cong0.3 \text{ at } 4.2°\text{K}.$$

We believe that the latter value of η is not inconsistent with the spectra given by Collins[13] for the compound in an applied magnetic field. It should be remarked here that if β were not approximately 90°, then the X axis would not lie in the plane containing the Z axis and local principal EFG axis, namely z. Moreover, the angle γ_q would then also be expected to vary with η [Eq. (7)]. For instance, if $\beta\cong45°$ and $\alpha\cong32°$ then $\gamma_q=19°$, with $\eta=0.7$, but $\gamma_q=8°$, with $\eta=0.3$.

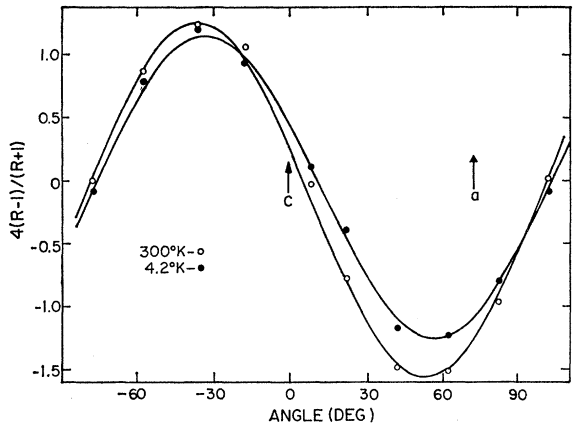

FIG. 2. Experimental data for transmission in the a-c plane. The angle is measured with respect to the c axis in the same sense as Φ of Fig. 1. The solid lines are calculated fits to the data.

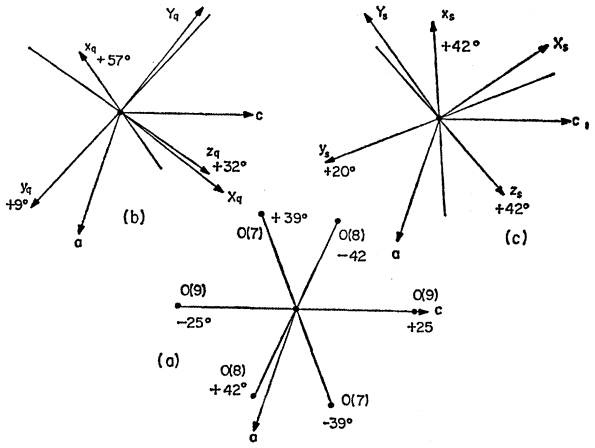

FIG. 3. Projection of the various axes upon the a-c plane showing the relationship between the octahedron (a), and sets of principal and local quadrupolar (b), and susceptibility (c) axes as defined in Fig. 1. Angles of projection above the plane are labeled (+) (one site shown). The principal axes X_s and Y_s are sometimes denoted by K_2 and K_1, respectively (Refs. 3 and 4).

IV. DISCUSSION

A. Relationship between the Local EFG Axes and Crystal Structure

The most recent crystal structure has been given by Montgomery *et al.*[10] The main result [Fig. 3(a)] is that, for one site, the iron ion is surrounded by a slightly distorted octahedron of water molecules, with one pair, O(9), at an angle of 25° with respect to the a-c plane and making a projection on the a-c plane which is essentially parallel to the c axis. The other two pairs, O(7) and O(8), lie roughly at angles of 39° and 42°, respectively, relative to the a-c plane. The three bonds are essentially at right angles to one another (89.3°, 91.2°, 90.9°) and of almost equal length [Fe-O(7):2.16 A, Fe-O(8):2.14 Å, and Fe-O(9):2.09 Å]. The second site (not shown) is obtained by reflection in the a-c plane. There is, of course, a fundamental ambiguity as to which set of EFG axes (x_q, y_q, z_q) goes with which site. The most reasonable choice is as shown in Fig. 3(b), in which the x_q axis points nearly in the direction of O(7), with the z_q axis nearly bisecting the angle between O(8) and O(9). As shown in the next section, this is in rough agreement with a simple rhombic crystal-field model, based upon the nearest-neighbor oxygens, and that deviations from it are due to the lower symmetry, that is, distortions of the octahedron, and the protons on the water molecules.[14]

[12] R. W. Grant, H. Wiedersich, A. H. Muir, Jr., U. Gonser, and W. N. Delgass, J. Chem. Phys. **45**, 1015 (1966).

[13] R. L. Collins and J. C. Travis, Bull. Am. Phys. Soc. **12**, 203 (1967); and (private communication).

[14] From the x-ray results one might expect a tetragonal model to be a good approximation with the axis of approximate symmetry directed towards O(9). The x and y axes could either point toward O(7) and O(8) or in between if there were a slight rhombic distortion.

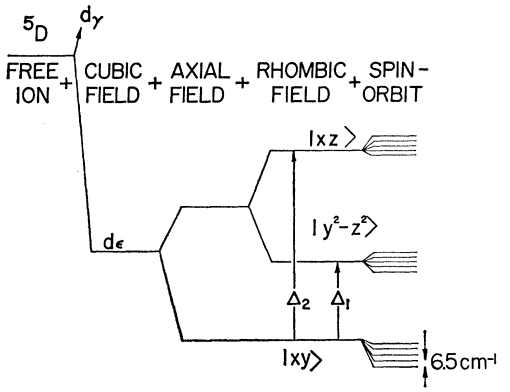

FIG. 4. Energy-level scheme for the Fe^{2+} ion in octahedral coordination.

Montgomery *et al.* do not give the proton positions, but from data on other Tutton salts[10] the protons are generally so located that the resulting dipole moments on the water molecules are directed at angles which bear little relationship to the axes of the basic octahedron itself. This problem has been discussed by Grimes and Webb.[15] One must, therefore, consider it somewhat fortuitous that the EFG axes are so closely related to the axes of the octahedron.

B. Crystal-Field Splittings

In an earlier paper[5] it was shown that a simple model of the crystal-field splittings of the Fe^{2+} orbitals, in which the states $|yz\rangle$ and $|xz\rangle$ were raised above $|xy\rangle$ by the amounts of Δ_1 and Δ_2, respectively, gave approximately the correct behavior of the quadrupole splitting of most ferrous compounds (Fig. 4). Since the y and z axes are directed in between the ligands, it is more reasonable for the middle orbital to be $|y^2-z^2\rangle$,[16] an assignment consistent with the susceptibility results (see Sec. IV C). Qualitatively, such a model works well here, for it yields a positive value for q providing Δ_1 and $\Delta_2 > kT$ and yields a value for η which is small at low temperatures and increases as kT approaches the value of Δ_1. A calculation of q and η then involves a thermal average of the EFG parameters for the various electronic levels and yields a quadrupole splitting:

$$\Delta E=\tfrac{1}{2}(e^2qQ)(1+\tfrac{1}{3}\eta^2)^{1/2}=(2/7)e^2Q(1-R)\langle r^{-3}\rangle F.$$

In this expression Q is the quadrupole moment of Fe-57, $(1-R)$ is the Sternheimer factor, and F is a complicated function of the crystal-field splittings, spin-orbit coupling constant λ, and temperature, which is generally evaluated by a computer. A recent work shows

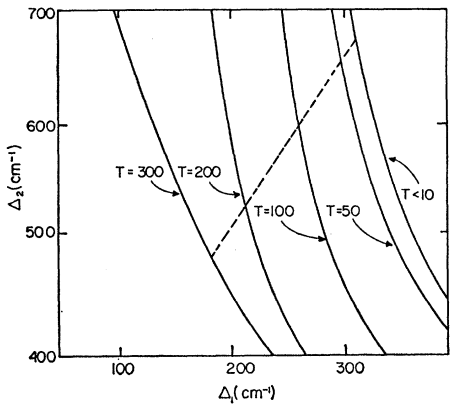

FIG. 6. Results of computer calculations: lines of constant quadrupole splitting at various temperatures for FAS, as a function of the crystal-field splittings. The dashed line gives the variation with temperature needed to explain experimental results with a rhombic model for the crystal field.

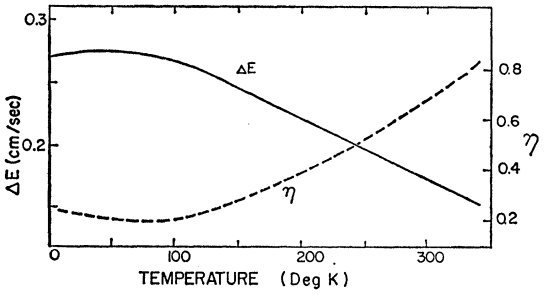

FIG. 5. Quadrupole splitting ΔE in FAS as compiled from experiment and fitted exactly in this work, and the EFG asymmetry parameter η as calculated.

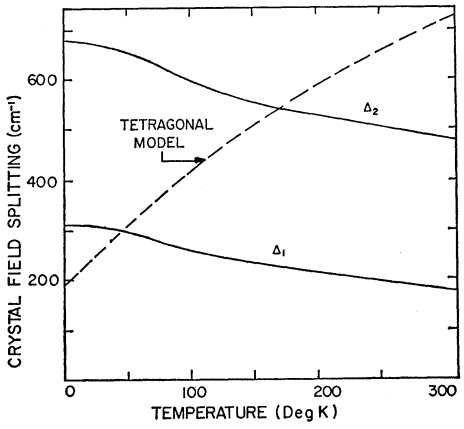

FIG. 7. Variation of the crystal-field splittings with temperature as a consequence of the assumed rhombic model and/or thermal expansion. The dashed line gives the splitting when one uses a simpler tetragonal model (Ref. 4).

[15] N. W. Grimes and H. F. Webb, Proc. Phys. Soc. (London) **82**, 1074 (1963).

[16] Either wave function $|yz\rangle$ or $|y^2-z^2\rangle$ is applicable for the middle orbital if there is a rhombic distortion. If the distortion is such that $|y^2-z^2\rangle$ is appropriate, it may be augmented by a small amount of the state $|3x^2-r^2\rangle$. In the absence of this admixture the EFG parameters have an identical dependence upon Δ_1 and Δ_2 for the two kinds of rhombic distortions.

that $(2/7)e^2Q(1-R)\langle r^{-3}\rangle \cong 0.4$ cm/sec for $FeSiF_6 \cdot 6H_2O$.[17] Adopting the same value for FAS, values of F versus T can be obtained from quadrupole-splitting measurements given in the literature[18]: $F \cong \Delta E/(0.4$ cm per sec) (Fig. 5). Using the computer, one can generate a family of curves of constant F which correspond to the experimental values at various temperatures varying only Δ_1 and Δ_2 (Fig. 6).[19] As pointed out previously,[5] these curves should intersect at a point if Δ_1 and Δ_2 are temperature-independent and the symmetry is purely rhombic. As shown, the curves do not intersect at a point. If one lets Δ_1 and Δ_2 vary with temperature one can follow a path (dotted line in Fig. 6) which gives roughly the proper values of η (Fig. 5) as well as the correct energy separation between the lowest two electronic states as measured by specific-heat or susceptibility studies.[1,3] Such a procedure yields $\Delta_1(T)$ and $\Delta_2(T)$, as shown in Fig. 7. Also shown are values of the splitting when one forces a purely tetragonal model to explain the susceptibilities.[4] We note that a much less extreme temperature dependence is required in the present analysis. It is thus quite likely that a model of yet lower symmetry than orthorhombic would yield even less temperature dependence. One must note, however, that the behavior we find for our rhombic splittings is compatible with thermal expansion; i.e., at higher temperatures, weaker fields.

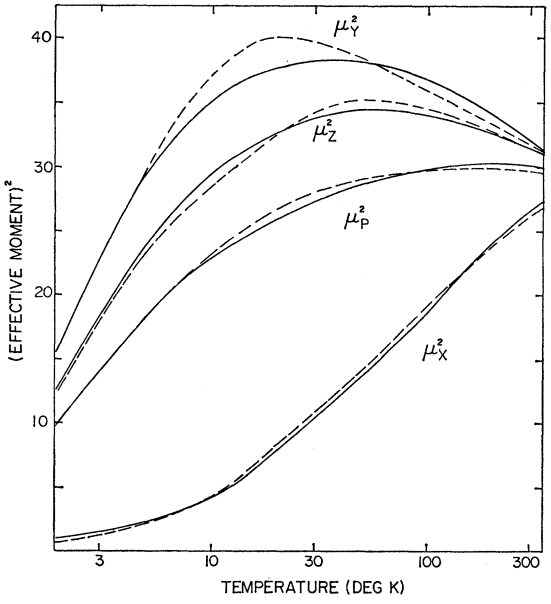

FIG. 8. Various (principal moments)^2 for FAS. Dashed lines are compiled from experiment. Solid lines are a fit based upon the crystal-field parameters but different orientations of the local susceptibility axes than for the local EFG axes.

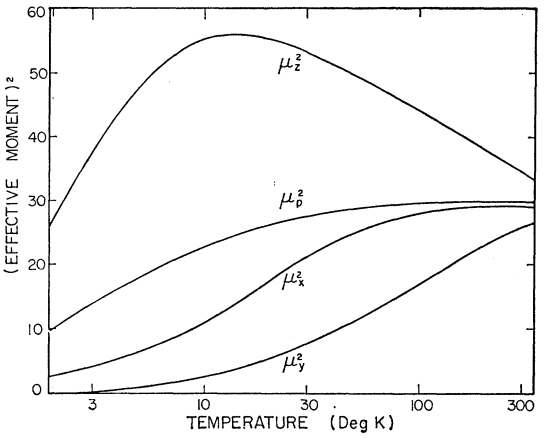

FIG. 9. (Local moments)^2 as calculated from the crystal-field splittings of Fig. 7. An orbital reduction factor of 0.95 is also assumed in obtaining these results.

The main point, however, is that the nature of the crystal-field splitting is consistent with the crystallographic data and yields values of the EFG parameters q and η which agree with those deduced from the experimental data on ΔE and the quadrupolar hyperfine anisotropy given in this work. There are sufficient uncertainties in both the theoretical calculations and the experimental data that an analysis in terms of a model exhibiting yet lower symmetry appears meaningless at present.

C. Paramagnetic Susceptibility

In many ways, the susceptibility tensor is similar to the EFG tensor. The local susceptibilities are calculated by performing appropriate thermal averages over the crystal-field states.[20] Moreover, as shown in the Appendix, the principal susceptibilities are the resultants of the local susceptibilities in much the same way as the quadrupolar hyperfine anisotropy is the resultant of the local Mössbauer absorption spectra from the individual sites. The chief difference lies in the fact that the principal X_s and Y_s axes of the susceptibility are, in general, rotated in the a-c plane with respect to the principal quadrupolar anisotropy axes X_q and Y_q. The angle between X_s and the c axis has been found to be $\sim 36°$,[6] whereas the angle between X_q and the c axis [Fig. 3(c)] is the negative of this value. In Fig. 8, we show a compilation of the available susceptibilities in the literature[2–4,6,21] graphed in terms of the effective

[17] A. J. Nozik and Morton Kaplan, Phys. Rev. **159**, 273 (1967). We use the following numbers for $FeSiF_6 \cdot 6H_3O$ at 4.2°K: $\Delta E = 0.37$ cm/sec and $F = 0.95$.

[18] See references listed in Ref. 5.

[19] Here we diagonalize a 15×15 matrix, that is, neglect effects of the d_γ orbitals. We also assume no $|3z^2-r^2\rangle$ admixture, the spin orbit constant $\lambda = 90\ \text{cm}^{-1}$, and the lattice contribution to the EFG is half as large as that assumed in Ref. 5 (but of the same sign).

[20] J. H. Van Vleck, *The Theory of Electric and Magnetic Susceptibilities* (Oxford University Press, London, 1932), p. 182.

[21] M. S. Jogelkar, Z. Krist. **98**, 411 (1938); A. Bose, Indian J. Phys. **22**, 483 (1948); S. Datta, *ibid.* **28**, 239 (1954); D. G. Thakurta and D. Mukhopadhyay, *ibid.* **40**, 69 (1966); T. Oktsuka (private communication). Professor Oktsuka has kindly informed us that the data for χ_1 and χ_3 in Ref. 3 were interchanged.

moments defined by $\mu_i^2=(3kT/N_0\beta^2)\chi_i$, where $N_0=$ Avogadro's number, β is the Bohr magneton, and χ_i are the various molar susceptibilities.

Using the crystal-field parameters of the previous section together with Van Vleck's formula[20] for the susceptibilities, we may calculate the values for the local effective moments μ_x^2, μ_y^2, μ_z^2, and $\mu_p^2=\frac{1}{3}(\mu_x^2+\mu_y^2+\mu_z^2)$ for the powder (Fig. 9). It is observed that μ_p^2 is in excellent agreement with experiment (solid line in Fig. 8). It is also observed that at low temperatures all three components differ widely, with the x and y components very small and z component large,[22] very much like the tetragonal model used by Bose *et al.*[4] and Ohtsuka *et al.*[3] Both works assumed that $\mu_\perp^2<\mu_{||}^2$, while the latter were forced to go to a rhombic model below about 20°K so that $\mu_{||}^2$ would decrease at lower temperatures, that is, the spin would be quenched. At higher temperatures all three components approach the spin-free behavior for $S=2$.

One may now go a step further and calculate the principal effective moments μ_X^2, μ_Y^2, and μ_Z^2 from the above local values μ_x^2, μ_y^2, and μ_z^2, using the results of the Appendix and the values of α and β as determined in Sec. III. The agreement with experiment (not shown) is reasonable. However, by permitting α and β for the local susceptibility axes to differ from the corresponding angles for the local EFG axes, we are able to improve the agreement with experiment (solid lines in Fig. 8). The angles that accomplish this are [Fig. 3(c)] $\alpha\cong 42°$ and $\beta\cong 117°$ with γ_s decreasing from $\sim -9°$ at 300°K to $\sim -3°$ at 4.2°K. Thus x_s, the axis which corresponds to the second largest component of the local susceptibility, in terms of the level scheme of Fig. 4, is essentially directed toward O(7), and z_s is again between O(8) and O(9).

It is not surprising if the systems (x_s, y_s, z_s) and (x_q, y_q, z_q) are different, since one is the result of diagonalizing a susceptibility tensor and the other the result of diagonalizing an EFG tensor.[23] Similar conclusions have been reached for the compound $FeCl_2\cdot 4H_2O$.[8,24] It must be remarked here, however, that we have not conclusively proved the local susceptibility axes to be as described above, since the orientations were deduced from calculated values based upon an oversimplified model. It is not completely impossible for these axes to coincide with *either* the local EFG axes *or* the octahedron axes.

V. CONCLUSIONS

We find that many of the simple ideas based upon crystal-field theory can account for the experimental description of the EFG and susceptibility tensors at the Fe^{2+} ion. However, certain discrepancies with experiment are obtained, using a rhombic model, which clearly demonstrates the effects of yet lower symmetry in this monoclinic compound.

ACKNOWLEDGMENTS

The authors would like to express their appreciation to the following for fruitful communications, suggestions, or aid during various stages of this work: P. Zory, S. A. Friedberg, B. Bleaney, T. Ohtsuka, P. Debrunner, H. Frauenfelder, J. Murphy and H. Shechter, G. M. Almy, E. C. Lingafelter, R. W. Grant, and R. L. Collins.

APPENDIX

In this section we present a derivation of the intensity ratio $R(\Theta, \Phi)$ as measured in the laboratory, but expressed in terms of the orientation of the local EFG axes for the two sites. This treatment is completely equivalent to that by Zory,[8] except that here it is done in a manner which brings out the similarity between the quadrupolar hyperfine anisotropy and the susceptibility.

For one site Zory[8] has shown that the intensity ratio for a thin absorber with isotropic recoilless fraction may be written

$$R=a_h/a_l$$
$$=\frac{4+K[(3\cos^2\vartheta-1)+\eta\sin^2\vartheta\cos 2\varphi]}{4-K[(3\cos^2\vartheta-1)+\eta\sin^2\vartheta\cos 2\varphi]}, \quad \text{(A1)}$$

where $K=(1+\frac{1}{3}\eta^2)^{-1/2}$ and the ϑ and φ are the usual spherical coordinates. Generalizing to two sites,

$$R=\Big(\sum_{i=1}^{2}\{4+K[(3\cos^2\vartheta_i-1)+\eta\sin^2\vartheta_i\cos 2\varphi_i]\}\Big)/\Big(\sum_{i=1}^{2}\{4-K[(3\cos^2\vartheta_i-1)+\eta\sin 2\vartheta_i\cos 2\varphi_i]\}\Big), \quad \text{(A2)}$$

where ϑ_i and φ_i are measured with respect to the local EFG axis system for each site, $i=1$ or 2. We now must write this expression in terms of the common spherical coordinates Θ and Φ (see Fig. 1). In principle, this may be accomplished using the $\mathfrak{D}$ rotation matrices of group theory,[25] since the angular terms are spherical harmonics of order 2, and are readily transformed. In order to discuss the susceptibility results on an equal basis, however, we find it more convenient to perform the usual coordinate transformation through the angles α, β, and γ as defined in Fig. 1, which shows the relation between the local axes (x, y, z) at site number 1 and the laboratory

[22] If $|xy\rangle$ is the ground state, then $|y^2-z^2\rangle$ must be the next higher orbital if μ_z^2 is to be largest, since the transformation from $|yz\rangle$ to $|y^2-z^2\rangle$ reverses the order of μ_y^2 and μ_z^2.

[23] The orientations of the local axes would then be expected to vary with temperature, a possibility not considered in this work.

[24] J. T. Schriempf and S. A. Friedberg, Phys. Rev. **136**, A518 (1964).

[25] D. M. Brink and G. R. Satchler, *Angular Momentum* (Oxford University Press, London, 1962).

axes (X, Y, Z). The required transformation for site number 1 is then

$$\begin{pmatrix} x \\ y \\ z \end{pmatrix} = T_1(\alpha, \beta, \gamma) \begin{pmatrix} X \\ Y \\ Z \end{pmatrix}, \tag{A3}$$

where

$$T_1(\alpha, \beta, \gamma) = \begin{pmatrix} \cos\beta\cos\gamma - \sin\alpha\sin\beta\sin\gamma & -\cos\beta\sin\gamma - \sin\alpha\sin\beta\cos\gamma & \cos\alpha\sin\beta \\ \sin\beta\cos\gamma + \sin\alpha\cos\beta\sin\gamma & -\sin\beta\sin\gamma + \sin\alpha\cos\beta\cos\gamma & -\cos\alpha\cos\beta \\ \cos\alpha\sin\gamma & \cos\alpha\cos\gamma & \sin\alpha \end{pmatrix}, \tag{A4}$$

with a similar transformation for the coordinates of the second site: $T_2(\alpha, \beta, \gamma) = T_1(\pi-\alpha, \beta, \gamma)$.[26] Using this transformation,

$$\begin{aligned} \sum_{i=1}^{2} [(3\cos^2\vartheta_i - 1) + \eta \sin^2\vartheta_i \cos 2\varphi_i] &= \sum_{i=1}^{2} [(3z_i^2 - 1) + \eta(x_i^2 - y_i^2)]/(x_i^2 + y_i^2 + z_i^2) \\ &= 2[A(\alpha, \beta, \gamma)(3Z^2 - 1) + B(\alpha, \beta, \gamma)(X^2 - Y^2)]/(X^2 + Y^2 + Z^2) \\ &= 2A(\alpha, \beta, \gamma)(3\cos^2\Theta - 1) + 2B(\alpha, \beta, \gamma)(\sin^2\Theta \cos 2\Phi), \end{aligned} \tag{A5}$$

where

$$A(\alpha, \beta) = 1 - \tfrac{1}{2}\cos^2\alpha(3 + \eta\cos 2\beta),$$

$$B(\alpha, \beta, \gamma_q) = [\eta\cos 2\beta - \tfrac{1}{2}\cos^2\alpha(3 + \eta\cos 2\beta)]\cos 2\gamma_q - \eta\sin\alpha\sin 2\beta\sin 2\gamma_q,$$

and

$$\tan 2\gamma_q = \frac{-\eta\sin\alpha\sin 2\beta}{\eta\cos 2\beta - \tfrac{1}{2}\cos^2\alpha(3 + \eta\cos 2\beta)}. \tag{A6}$$

The angle γ_q has been defined above so that the term in XY, which comes from the transformation, vanishes. Thus, we chose a set of principal axes (X, Y, Z), the quadrupolar hyperfine anisotropy axes, so that the ratio $R(\Theta, \Phi)$ has a simple form:

$$R(\Theta, \Phi) = \frac{4 + K[A(3\cos^2\Theta - 1) + B\sin^2\Theta\cos 2\Phi]}{4 - K[A(3\cos^2\Theta - 1) + B\sin^2\Theta\cos 2\Phi]}. \tag{A7}$$

We may also use the above transformation matrices to transform the local susceptibility tensors to the corresponding principal-axes system for the susceptibility:

$$\chi = \tfrac{1}{2}(\tilde{T}_1\chi_1 T_1 + \tilde{T}_2\chi_2 T_2), \tag{A8}$$

where

$$\chi_1 = \chi_2 = \begin{pmatrix} \chi_x & 0 & 0 \\ 0 & \chi_y & 0 \\ 0 & 0 & \chi_z \end{pmatrix}$$

and

$$\chi = \begin{pmatrix} \chi_X & 0 & 0 \\ 0 & \chi_Y & 0 \\ 0 & 0 & \chi_Z \end{pmatrix}. \tag{A9}$$

One then obtains the following in terms of χ_z, $\chi_+ = \chi_x + \chi_y$ and $\chi_- = \chi_x - \chi_y$:

$$\begin{aligned} \chi_Z &= \chi_z - \tfrac{1}{2}\cos\alpha(2\chi_z - \chi_+ + \chi_-\cos 2\beta), \\ \chi_X + \chi_Y &= \chi_+ + \tfrac{1}{2}\cos^2\alpha(2\chi_z - \chi_+ + \chi_-\cos 2\beta), \\ \chi_X - \chi_Y &= [\chi_-\cos 2\beta - \tfrac{1}{2}\cos^2\alpha(2\chi_z - \chi_+ + \chi_-\cos 2\beta)] \\ &\quad \times \cos 2\gamma_s - \chi_-\sin\alpha\sin 2\beta\sin 2\gamma_s, \end{aligned} \tag{A10}$$

and

$$\tan 2\gamma_s = \frac{-\chi_-\sin\alpha\sin 2\beta}{\chi_-\cos 2\beta - \tfrac{1}{2}\cos^2\alpha(2\chi_z - \chi_+ + \chi_-\cos 2\beta)}. \tag{A11}$$

The condition on γ_s is chosen to diagonalize the principal susceptibility tensor χ, that is, to eliminate the XY cross terms.

[26] The order of rotation (Fig. 1) is first by γ about the Z axis, then by $(\frac{1}{2}\pi - \alpha)$ about X', and finally by β about z.